

A Learning-Based QoE-Driven Spectrum Handoff Scheme for Multimedia Transmissions over Cognitive Radio Networks

Yeqing Wu, Fei Hu, *Member, IEEE*, Sunil Kumar, *Senior Member, IEEE*, Yingying Zhu, *Member, IEEE*, Ali Talari, Nazanin Rahnavard, *Member, IEEE*, and John D. Matyjas, *Senior Member, IEEE*

Abstract—Enabling the spectrum handoff for multimedia applications in cognitive radio networks (CRNs) is challenging, due to multiple interruptions from primary users (PUs), contentions among secondary users (SUs), and heterogeneous Quality-of-Experience (QoE) requirements. In this paper, we propose a learning-based and QoE-driven spectrum handoff scheme to maximize the multimedia users' satisfaction. We develop a mixed preemptive and non-preemptive resume priority (PRP/NPRP) M/G/1 queueing model for modeling the spectrum usage behavior for prioritized multimedia applications. Then, a mathematical framework is formulated to analyze the performance of SUs. We apply the reinforcement learning to our QoE-driven spectrum handoff scheme to maximize the quality of video transmissions in the long term. The proposed learning scheme is asymptotically optimal, model-free, and can adaptively perform spectrum handoff for the changing channel conditions and traffic load. Experimental results demonstrate the effectiveness of the proposed queueing model for prioritized traffic in CRNs, and show that the proposed learning-based QoE-driven spectrum handoff scheme improves quality of video transmissions.

Index Terms—Cognitive Radio Networks, Spectrum Handoff, Queueing Model, QoE, Reinforcement Learning, Multimedia Transmission.

I. INTRODUCTION

WIRELESS multimedia applications are rapidly growing, leading to the increased demand for RF spectrum. The fixed frequency allocation policies in wireless networks limit the spectrum resources available for multimedia applications [1]. Recently, the cognitive radio networks (CRN) have become attractive as they can enhance spectrum utilization and provide high bandwidth through dynamic spectrum allocation (DSA) [2].

Manuscript received 5 January 2014; revised 7 May 2014. This work was supported by the U.S. Department of Defense under Grant No. FA8750-11-1-0048 and 8750-13-1-046, and NSF grant CCF-1439182. Approved for public release by DOD; Distribution Unlimited: 88ABW-2014-3099, 26 June 2014. This work was presented in part at the IEEE GlobalSIP Conference, 2013.

Y. Wu and F. Hu are with the Electrical and Computer Engineering, University of Alabama, Tuscaloosa, AL 35487, USA (e-mail: ywu40@ua.edu, fei@eng.ua.edu).

S. Kumar is with the Electrical and Computer Engineering, San Diego State University, San Diego, CA 92182, USA (e-mail: skumar@mail.sdsu.edu).

Y. Zhu is with the Electrical and Computer Engineering, University of California, Riverside, CA 92507, USA (e-mail: yzhu010@ucr.edu).

A. Talari is with the Electrical and Computer Engineering, Oklahoma State University, Stillwater, OK, 74075, USA (e-mail: ali.talari@okstate.edu).

N. Rahnavard is with the Electrical Engineering and Computer Science Department, University of Central Florida, Orlando, FL, 32816, USA (e-mail: nazanin@eecs.ucf.edu).

J. D. Matyjas is with Air Force Research Laboratory, Rome, NY 13441, USA (e-mail: john.matyjas@us.af.mil).

Digital Object Identifier 10.1109/JSAC.2014.141115.

In CRN, when a primary user (PU) reappears on a channel, existing secondary user(s) (SUs) must return the channel control to it and find other unoccupied spectrum band(s) to switch (i.e., handoff). Randomness of PU arrivals and uncertain channel conditions, however, make the smooth spectrum handoff difficult, which may lead to performance degradation of SUs. In order to meet the bandwidth requirements of SUs, spectrum usage behaviors in CRNs need to be analyzed, and spectrum handoff strategies should be designed carefully.

Spectrum handoff schemes can be categorized into three types: *proactive*, *reactive* and *hybrid* [3]. In the *proactive* spectrum handoff, SUs utilize the knowledge of PU traffic model to predict PUs' activities, decide the target channels, and perform channel switching before the reappearance of PUs. Thus, the handoff delay of the proactive scheme is usually very small. However, an accurate PU traffic model is a key design factor in this type of handoff schemes. In the *reactive* spectrum handoff, an SU performs spectrum sensing to find target channel(s) after being interrupted by a PU. Such a scheme can obtain accurate channel status for handoff. However, spectrum sensing on a wide spectrum may introduce handoff delay. The *Hybrid* spectrum handoff scheme combines the reactive and proactive schemes by using the proactive spectrum sensing and reactive handoff action [3]. It can achieve a fast spectrum handoff since spectrum sensing is not performed in an on-demand manner.

Supporting the multimedia applications in CRN is challenging because of PU interruptions, SU contentions, and heterogeneous Quality-of-Experience (QoE) requirements, etc. In order to analyze the effects of PU interruptions and SU contentions on spectrum handoff, we propose a mixed preemptive and non-preemptive resume priority (PRP/NPRP) M/G/1 queueing model to manage and characterize spectrum usage behavior of PUs and SUs. In the proposed queueing model, the queueing between the PUs and SUs is modeled with PRP M/G/1 queueing model to ensure that PUs have preemptive control over the assigned channels. And the queueing among SUs is modeled with NPRP M/G/1 queueing model to prevent an SU from interrupting the ongoing transmission of other SUs. This queueing model preserves the overall delay performance of SUs by avoiding frequent spectrum handoffs due to the interruptions from other SUs, which may occur when using the queueing model of [4], [5]. Furthermore, the queueing model of [6]–[8] assumes that all SUs have the same priority; this makes their queueing models unsuitable when some SUs

have more stringent delay constraints than others. To support multimedia applications, we prioritize SUs according to their QoE requirements, and our mixed queueing model provides a better performance for SU applications with higher priorities by allocating more available network resource to them.

Existing spectrum handoff schemes aim to reduce the SU transmission delay caused by spectrum handoff [5], [6], [9], [10]. However, they seldom consider the effects of other channel conditions (e.g., the packet error rate (PER)). To enhance the quality of multimedia applications, it is important to consider both the transmission delay and the transmission channel quality, when choosing channels for spectrum handoff.

The QoE has been recently studied for multimedia transmissions. The mean opinion score (MOS) is a major metric of QoE, which is a direct measurement of end-user satisfaction [11]. In this paper, we propose a novel QoE-driven spectrum handoff scheme that aims to enhance the end-user satisfaction, by choosing the available channel with maximum expected MOS for spectrum handoff.

Besides, the existing spectrum handoff schemes choose the spectrum for handoff in a *myopic* manner [5]–[10], [12], [13], [26]–[28]. They greedily choose the spectrum with the maximum immediate rewards for handoff, without considering the influence of the current action on the future state. Since the network status in CRN is time-varying and evolves over time and space, the greedy policy may not achieve the optimal rewards in the long term. In order to achieve the asymptotically optimal rewards in the long term, we propose the use of reinforcement learning in our QoE-driven spectrum handoff scheme. The proposed scheme utilizes the current observed CRN state, the knowledge from the previous spectrum handoff operations, and the past channel conditions.

A. Main Contributions

The main contributions of this paper are three-fold:

1) A mixed PRP/NRP M/G/1 queueing model is developed for spectrum handoff to provide differentiated service. This model explicitly considers the effect of different channel conditions (such as multiple PUs' interruptions, SUs' contentions, the general distribution of the service time, and prioritized traffic) on the performance of spectrum handoff. It can overcome the problem of overly frequent spectrum handoffs or un-differentiated service of other queueing models. Our queueing model is flexible and can be extended to other utility evaluation functions.

This part of work is extended from our prior work [12], but we give more detailed analysis in this paper and also include the analysis of imperfect sensing.

2) A QoE-driven spectrum handoff scheme is proposed, which maximizes the quality for the prioritized multimedia users. The proposed scheme explicitly considers complex CRN conditions, including multiple interruptions, heterogeneous QoE requirement of SUs, channel contentions among multiple SUs, and packet drop rate (PDR) due to handoff delay and channel PER. To the best of our knowledge, no previous spectrum handoff scheme has considered the QoE requirements from heterogeneous multimedia SUs.

3) A reinforcement learning-based QoE-driven spectrum handoff scheme is proposed to adaptively perform spectrum

handoff under the changing channel conditions and traffic loads by learning from previous spectrum handoffs and past channel conditions. The proposed learning scheme is asymptotically optimal, model-free, and can adaptively perform spectrum handoff under the changing CRN conditions. It can overcome the myopic problem of other spectrum handoff schemes.

The rest of this paper is organized as follows. The related schemes are briefly discussed in Section II. Section III describes the network assumptions and introduces the proposed mixed PRP/NRP M/G/1 queueing model. Section IV provides the mathematical analysis of the expected handoff delay and delivery time of SU connections. Section V describes the proposed QoE-driven spectrum handoff scheme, followed by the application of reinforcement learning in Section VI. Simulation results are presented in Section VII, followed by conclusions in Section VIII.

II. RELATED WORK

For *proactive* spectrum handoff, Yoon *et al.* [9] proposed a voluntary spectrum handoff to minimize SU disruption periods. Song and Xie [10], [14] proposed a proactive spectrum handoff framework by using discrete-time Markov chain in CR ad hoc networks. In this approach, SUs used the observed channel usage statistics to vacate a channel before a PU returns, to avoid unwanted interference. In order to reduce the communication disruptions to PUs and increase the channel utilization efficiency, Zheng *et al.* [15] proposed the optimal target channel sequence selection scheme for proactive spectrum handoff with Poisson arriving PUs.

For *reactive* spectrum handoff, Zhang *et al.* [16] investigated the performance of the opportunistic spectrum access schemes. Guipponi *et al.* [17] proposed a fuzzy-based spectrum handoff algorithm, which allowed the SUs to use the spectrum while ensuring that the aggregate interference to PUs does not exceed a certain threshold. In [18], the authors investigated the performance of CRNs by considering the realistic channel handoff agility, where the interrupted SUs can switch only to their neighboring channels.

Existing spectrum handoff schemes assume that all SUs have the same priority, and focus on reducing the SU transmission delay, while ignoring other important QoS/QoE parameters and channel quality. This may make them unsuitable for multimedia applications with different delay constraints. Also, these spectrum handoff schemes select the channel for handoff in a myopic manner; they greedily choose the channel(s) with the maximum immediate reward, without considering its impact on the future status and rewards. The Queueing models for prioritized SU applications were considered in [4] and [19]. However, these models allow SU applications with higher priorities to preempt SU applications with lower priorities. This may deteriorate the average delay performance of CRNs due to frequent spectrum handoffs, especially when the network is busy.

III. NETWORK MODEL

In this paper, we consider a CRN with M independent channels; each channel is allocated to a PU [6]. At any time,

only one user can transmit its data over a channel. During its transmission period, a SU connection may experience multiple interruptions from PUs. In order to overcome the contention for the same channel among multiple SUs, a distributed channel selection scheme is adopted in [10], which uses the same seed to generate a pseudo-random channel selecting sequence.

We assume that each SU is equipped with two transceivers (one for transmission and the other for sensing) as in [10], [20]. The sensing transceiver has two major functions [10], [20]: 1) observe the channel usage and store the channel statistics in memory for predicting the future channel availability; 2) confirm that the newly selected channel is idle for SU transmission. We assume that SUs can sense the existence of PUs as in [4]. The common hopping is used for the spectrum coordination among the PUs and SUs.

In our network model, an SU performs handoff to other channel only when a PU appears in the current channel, as recommended in the IEEE 802.22 standard [21]. Thus, the selection of the target channel candidate set is performed proactively, and the spectrum handoff action is performed reactively in our scheme. Thus, it can be called as hybrid spectrum handoff scheme, which combines reactive and proactive schemes by using proactive spectrum sensing and reactive handoff action [3].

A. Mixed PRP/NPRP Queueing Network Model

We use a PRP M/G/1 queueing model to characterize the spectrum usage behavior of the PU and SU connections. A NPRP M/G/1 queue is used to model the spectrum usage behavior between SU connections. In this model, an ongoing SU is allowed to complete its service without being interrupted by other SUs, regardless of their priority. This strategy improves the average throughput for SUs by avoiding frequent spectrum handoffs between SUs.

To support multimedia applications, the queueing model prioritizes SUs according to their QoE requirements. Each channel maintains one priority queue for each prioritized user group in order to avoid the well-known head-of-line blocking effect [22], [23]. Specifically, $Q_p^{(k)}$ is the primary queue for the PU at channel k , and $Q_j^{(k)}$ is the queue for SUs with priority j at channel k , $1 \leq j \leq N$, where N is the number of SU priority levels. Priority $j = 1$ ($j = N$) is the highest (lowest) priority for SUs. The SU connections of the same priority follow the policy of first-come-first-served (FCFS). By not allowing SUs with lower priorities to transmit before the enqueued SUs with higher priorities in a channel, the proposed queueing model provides more channel access opportunities to the higher-priority SUs.

When a PU arrives, the ongoing SU is interrupted and it needs to decide to either stay at the current channel or switch to another one. If the SU chooses to stay at the current channel, it is placed at the head of the queue of its priority. If the SU chooses to switch to another channel, it is pushed at the tail of the corresponding priority queue in the channel.

As shown in Fig. 1, a PU is transmitting over channel k in the beginning, and its transmission will be completed without interruption. An SU with priority j is transmitting over

TABLE I
MAIN PARAMETERS FOR QUEUEING ANALYSIS

Symbol	Meaning
$\lambda_j^{(k)}$	Arrival rate of a user with priority j at channel k
$\mu_j^{(k)}$	Service rate of a user with priority j at channel k
$E[X_j^{(k)}]$	First moment of service time for a user with priority j at channel k
$E[N_j^{(k)}]$	Average number of users with priority j in queue $Q_j^{(k)}$ at channel k
$\rho_j^{(k)}$	Normalized load of channel k due to a user with priority j at channel k , where $\rho_j^{(k)} = \lambda_j^{(k)} E[X_j^{(k)}]$
$\omega_{j,i}^{(k)}$	Arrival rate of a type- (j, i) SU connection at channel k . $\omega_{j,0}^{(k)} = \lambda_j^{(k)}$
$\Phi_{j,i}^{(k)}$	Effective service time of a type- (j, i) SU connection, which is the valid transmission time for a SU connection with priority j between its i^{th} and the $(i+1)^{th}$ interruptions at channel k . $E[\Phi_{j,0}^{(k)}] = E[X_j^{(k)}]$
$\rho_{j,i}^{(k)}$	Normalized load of channel k due to a type- (j,i) SU at channel k

channel k' . When interrupted by a PU, this SU will either stay at k' or switch to another channel. If the SU chooses to stay at k' , as shown by the “No” branch following the “Switch” box in Fig. 1, it is pushed at the head of $Q_j^{(k')}$. If it switches to channel k (as shown by the “Yes” branch after the “Switch”), it is pushed back to the tail of $Q_j^{(k)}$.

IV. QUEUEING ANALYSIS OF SPECTRUM HANDOFF

Priority queueing analysis of the expected delay performance over time is critical for a delay-sensitive spectrum handoff scheme. In this section, we describe a mathematical framework to evaluate the delay performance of the proposed queueing model. We assume that the arrival processes of PU and SU follow Poisson distribution as in [4], [6]. The SU connection with priority j that is experiencing its i^{th} interruption is denoted as the type- (j, i) SU connection, where $i \geq 0$. The main parameters of the queueing model used in the analysis are listed in Table I.

A. Analysis of Expected Handoff Delay

When a SU is interrupted, it can stay at the current channel or switch to another available channel. We call the first case as the *staying* case and the second one as the *switching* case. To choose the optimum handoff behavior for the interrupted SU, the expected MOS of target channels and thus the expected handoff delay of choosing each available channel need to be estimated. We now provide a mathematical model to analyze the expected handoff delay for different cases.

We denote the interrupted SU connection with priority j as SU_j , and consider seven types of user connections at the target channel which may affect the expected handoff delay of SU_j :

- 1) PU_a : newly arriving PU connection at the target channel.
- 2) U_c : denotes the PU or SU of any priority, which is currently using the target channel.
- 3) PU_{old} : PUs in the queue at the target channel.
- 4) SU_H : set of SUs (with priorities higher than j) in the queue that arrive before the SU_j at the target channel.

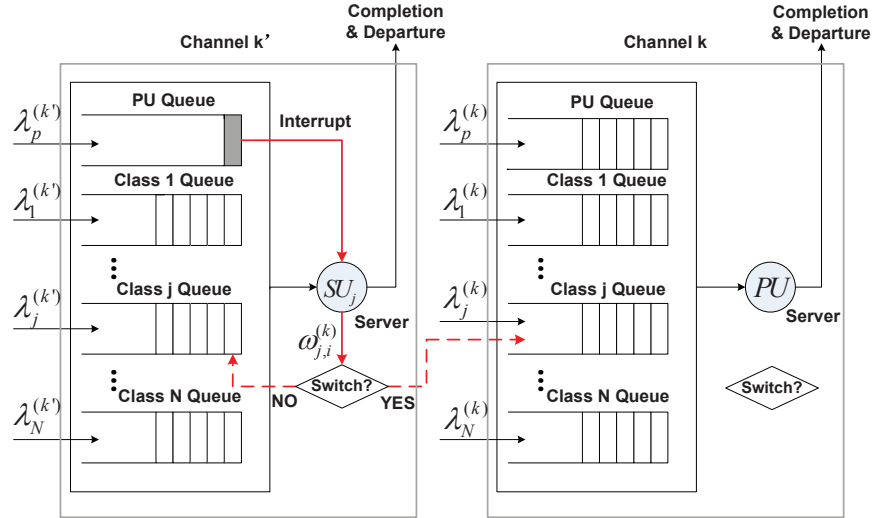


Fig. 1. Queuing scheme for handling spectrum handoff in the mixed PRP/NPRP M/G/1 queueing model. (For simplicity of representation, only two channels are shown here.) [12]

- 5) SU_j : set of SUs in the queue $Q_j^{(k)}$ that arrived at the target channel before interruption.
- 6) PU_{new} : set of PUs that arrive at the target channel after the interruption while SU_j is still waiting in queue.
- 7) $SU_{new,H}$: set of SU connections with priorities higher than j , that arrived at the target channel after the interruption while SU_j is queued at the target channel.

Fig. 2 shows an example of spectrum handoff when multiple interruptions occur during the transmission period of SU_j . In the beginning, SU_j is using the channel CH1. Each time the SU is interrupted by a PU, it chooses the best available channel (i.e., with the best expected MOS) for handoff. At the first interruption, we assume CH2 is the best available channel and the SU connection switches to it. Since it is idle, the handoff delay equals to the switch time t_s . At the second interruption, SU_j decides to stay at CH2 and is pushed at the head of queue $Q_j^{(2)}$; it waits for completion of the service of PU_a and already queued SU_H . At the third interruption, CH1 is chosen, which is serving an existing user U_c . Thus, SU_j is pushed at the tail of queue $Q_j^{(1)}$. SU_j will not gain channel access until U_c and SU_H complete their transmission. For each interruption, PU_{new} and $SU_{new,H}$ need to be estimated when choosing the best available channel (we discuss this in detail below).

Theorem 1. Let the handoff delay $E[D_{j,i}^{(k)}]$ be the time duration from the instant the i^{th} interruption occurs to the instant the interrupted transmission is resumed, assuming channel k is chosen for spectrum handoff. It is calculated as

$$E[D_{j,i}^{(k)}] = \begin{cases} E[W_j^{(k)}], & \text{if } c_{i-1} = c_i = k \\ E[W_j^{(k)}] + t_s, & \text{if } (c_{i-1} = k') \neq (c_i = k) \end{cases}, \quad (1)$$

where

$$E[W_j^{(k)}] = \frac{\prod_{\ell=1}^{j-1} (1 - \rho_p^{(k)} - \sum_{n=1}^{\ell-1} \rho_n^{(k)} + \sum_{i=0}^{I_{max}} \rho_{\ell,i}^{(k)})}{\prod_{\ell=1}^j (1 - \rho_p^{(k)} - \sum_{n=1}^{\ell-1} \sum_{i=0}^{I_{max}} \rho_{n,i}^{(k)})} E[X_p^{(k)}]. \quad (2)$$

and

$$E[W_j^{(k)}] = \frac{(1 - \rho_p^{(k)})(E[R^{(k)}] + \frac{(\lambda_p^{(k)})^2 E[(X_p^{(k)})^2]}{2(1 - \lambda_p^{(k)} E[X_p^{(k)}])} E[X_p^{(k)}])}{(1 - \rho_p^{(k)} - \sum_{n=1}^{j-1} \sum_{i=0}^{I_{max}} \rho_{n,i}^{(k)})(1 - \rho_p^{(k)} - \sum_{n=1}^j \sum_{i=0}^{I_{max}} \rho_{n,i}^{(k)})}. \quad (3)$$

In the above equations, c_i denotes the target channel for spectrum handoff at i^{th} interruption. $E[W_j^{(k)}$] (or $E[W_j^{(k)}$]) denote the average waiting time of the i^{th} interruption if SU_j chooses to stay at the current channel (switches to channel k). Since the switching time t_s is assumed to be known, we now describe how to calculate $E[W_j^{(k)}$] and $E[W_j^{(k)}$].

Proof. We assume that SUs can detect the existence of PUs as in [6]. Estimating the expected handoff delay for the two cases involves the estimation of expected PU waiting time during the interruption. We discuss below the formulae for PU and SU waiting times.

1) *PU Waiting Time:* The expected waiting time for a PU connection at channel k depends on the residual service time of the ongoing PU connection and the average number of PU connections in the primary queue. Let $\lambda_p^{(k)}$ be the PU arrival rate, and $E[X_p^{(k)}]$ be the average service time of the PU at channel k . Let $E[R_p^{(k)}]$ be the mean residual time for the ongoing PU connection at channel k , and $E[N_p^{(k)}]$ be the average number of PU connections waiting in the queue. From [23], we can get the expected PU waiting time $E[W_p^{(k)}]$ and the average number of PU connections $E[N_p^{(k)}]$, waiting in the primary queue at channel k as [12]

$$E[W_p^{(k)}] = \frac{E[R_p^{(k)}]}{1 - \rho_p^{(k)}} = \frac{\lambda_p^{(k)} E[(X_p^{(k)})^2]}{2(1 - \lambda_p^{(k)} E[X_p^{(k)}])}, \quad (4)$$

where $\rho_p^{(k)} = \lambda_p^{(k)} E[X_p^{(k)}]$.

$$E[N_p^{(k)}] = \lambda_p^{(k)} E[W_p^{(k)}] = \frac{(\lambda_p^{(k)})^2 E[(X_p^{(k)})^2]}{2(1 - \lambda_p^{(k)} E[X_p^{(k)}])}. \quad (5)$$

2) *SU Waiting Time:* We consider the expected SU waiting time for two cases.

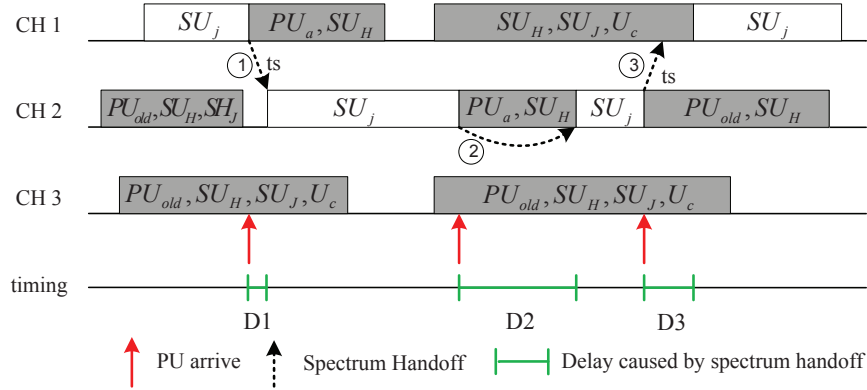


Fig. 2. An example of the transmission process for a SU connection experiencing multiple interruptions. For simplicity, we assume there are only 3 channels available to the SU of interest. t_s is the channel switching time.

a) *Staying Case:* In this case, the SU connection with priority j chooses to stay at the current operating channel, e.g. $c_i = c_{i-1} = k$. As shown in Figs. 1 and 2, after being pushed back into the queue $Q_j^{(k)}$, it must wait until all the traffic of PU_a , SU_H , PU_{new} and $SU_{new,H}$ at channel k are served. Thus, the value of $E[W_j^{(k)}]$ consists of three parts: the service time of the arriving PU, service time of SU_H and service time of newly arriving users PU_{new} and $SU_{new,H}$.

Let $E[W_{SU_H}^{(k)}]$ be the expected cumulative waiting time resulting from the queueing SU connections with higher priorities at channel k , and $E[W_{new}^{(k)}]$ be the cumulative waiting time caused by newly arriving PU and SU connections with higher priorities during the i^{th} interruption. We can obtain the average waiting time $E[W_j^{(k)}]$ as in Eq. 6 (top of next page) where $\lambda_p^{(k)} E[W_j^{(k)}] E[X_p^{(k)}]$ and $\sum_{n=1}^{j-1} \sum_{i=0}^{I_{max}} \omega_{n,i}^{(k)} E[W_j^{(k)}] E[\Phi_{n,i}^{(k)}]$ are the cumulative service time for the newly arriving users PU_{new} and $SU_{new,H}$ (please refer to Fig. 2 for different types of PUs and SUs). $E[\Phi_{n,i}^{(k)}]$ is the expected service time for a type- (n, i) SU connection, which represents the expected transmission duration of a secondary connection with priority n between its i^{th} and $(i+1)^{th}$ interruptions. If the general distributions of the service time of PU and SUs without interruption ($i=0$) are known as system parameters in advance, the distribution of $\Phi_{n,i}^{(k)}$ and thus its expectation, for any $i > 0$, can be derived following the Appendix B in [6].

With Little's theorem $E[N] = \lambda E[W]$ and the normalized load $\rho = \lambda E[X]$, we can rewrite (6) as

$$E[W_j^{(k)}] = \frac{E[X_p^{(k)}] + \sum_{n=1}^{j-1} \sum_{i=0}^{I_{max}} \rho_{n,i}^{(k)} E[W_n^{(k)}]}{1 - \rho_p^{(k)} - \sum_{n=1}^{j-1} \sum_{i=0}^{I_{max}} \rho_{n,i}^{(k)}}. \quad (7)$$

where $E[W_n^{(k)}]$ denotes the average waiting time of the SU_n connection with a higher priority, where $1 \leq n \leq j-1$.

Then, using the induction method, we can obtain the general expression of $E[W_j^{(k)}]$ as in (2).

b) *Switching Case:* In this case, the interrupted SU connection with priority j chooses to switch from channel $c_{i-1} = k'$ to another channel (e.g., $c_i = k$). After the switch, it must wait in the tail of $Q_j^{(k)}$, until all the traffic

of U_c , PU_{old} , SU_H , SU_J , PU_{new} and $SU_{new,H}$ are served. We denote $E[W_j^{(k)}]$ as the waiting time for the interrupted SU connections with priority j at channel k . Hence, we have $E[D_{j,i}^{(k)}] = E[W_j^{(k)}] + t_s$.

The average residual service time $E[R^{(k)}]$ of the ongoing connection (U_c) at channel k can be represented as [23]:

$$E[R^{(k)}] = \frac{1}{2} \lambda_p^{(k)} E[(X_p^{(k)})^2] + \frac{1}{2} \sum_{j=1}^N \sum_{i=0}^{I_{max}} \omega_{j,i}^{(k)} E[(\Phi_{j,i}^{(k)})^2]. \quad (8)$$

Let $E[W_Q^{(k)}]$ be the expected service time of the enqueued PU_{old} , SU_H and SU_J . And let $E[W_{new}^{(k)}]$ be the service time of the newly arriving PU connections (PU_{new}) and SU connections ($SU_{new,H}$). The $E[W_j^{(k)}]$ can be expressed as Eq. 9 (next page), where $E[N_{j,i}^{(k)}]$ is the average number of the type- (j, i) SU connections which are queueing in queue $Q_j^{(k)}$ at channel k . $E[N_p^{(k)}] E[X_p^{(k)}]$ is the cumulative service time of PUs which are already in the primary queue of channel k at the moment of handoff. Other symbols in (9) have the same meaning as those in the staying case.

By using Little's theorem, we can rewrite (9) as

$$E[W_j^{(k)}] = \frac{E[R^{(k)}] + E[N_p^{(k)}] E[X_p^{(k)}] + \sum_{n=1}^{j-1} \sum_{i=0}^{I_{max}} \rho_{n,i}^{(k)} E[W_n^{(k)}]}{1 - \rho_p^{(k)} - \sum_{n=1}^j \sum_{i=0}^{I_{max}} \rho_{n,i}^{(k)}}. \quad (10)$$

where $E[W_n^{(k)}]$ denotes the average waiting time of the SU_n connection with a higher priority, where $1 \leq n \leq j-1$.

By using the induction method, we can obtain the general expression of $E[W_j^{(k)}]$ as in (3). \square

B. Analysis of Expected Delivery Time

With traffic-adaptive target channel selection for spectrum handoff, the expected delivery time can be used to evaluate the performance of the proposed queueing model.

The expected delivery time of a SU connection, which experiences n interruptions during transmission, consists of the expected delays caused by interruptions and its service

$$E[W_j^{(k)}] = E[X_p^{(k)}] + E[W_{SU_H}^{(k)}] + E[W_{new}^{(k)}], \quad (6)$$

$$\text{where } E[W_{SU_H}^{(k)}] = \sum_{n=1}^{j-1} \sum_{i=0}^{I_{max}} E[N_{n,i}^{(k)}] E[\Phi_{n,i}^{(k)}],$$

$$E[W_{new}^{(k)}] = \lambda_p^{(k)} E[W_j^{(k)}] E[X_p^{(k)}] + \sum_{n=1}^{j-1} \sum_{i=0}^{I_{max}} \omega_{n,i}^{(k)} E[W_j^{(k)}] E[\Phi_{n,i}^{(k)}],$$

$$E[W_j^{(k)}] = E[R^{(k)}] + E[W_Q^{(k)}] + E[W_{new}^{(k)}], \quad (9)$$

$$\text{where } E[W_Q^{(k)}] = E[N_p^{(k)}] E[X_p^{(k)}] + \sum_{n=1}^j \sum_{i=0}^{I_{max}} E[N_{n,i}^{(k)}] E[\Phi_{n,i}^{(k)}],$$

$$E[W_{new}^{(k)}] = \lambda_p^{(k)} E[W_j^{(k)}] E[X_p^{(k)}] + \sum_{n=1}^{j-1} \sum_{i=0}^{I_{max}} \omega_{n,i}^{(k)} E[W_j^{(k)}] E[\Phi_{n,i}^{(k)}],$$

time. Since the service time of SU connections is assumed to be known, we only need to estimate its expected delay for estimating its expected delivery time.

When $i > I_{max}$, we drop the packet. This results in $D_{j,i}^{(k)} = 0$. The probability that the type-(j,i) SU connection will be interrupted is $P_{j,i}^{(k)} = \lambda_p^{(k)} E[\Phi_{j,i}^{(k)}]$ [6]. Thus, the expected delay of a SU connection with priority j can be derived as

$$E[Delay_j] = \sum_{i=0}^{I_{max}} i P_{j,i}^{(k)} E[D_{j,i}^{(k)}]. \quad (11)$$

where $E[D_{j,i}^{(k)}]$ is the handoff delay as described in (1).

C. Imperfect Sensing

In this section, based on the effects of imperfect sensing as described in [24], we discuss how to integrate the imperfect sensing (i.e., false alarm and miss detection) into our spectrum handoff scheme.

Miss detection occurs when the actual channel state is in *busy* state but the prediction channel state is in *idle* state. This will cause SUs to send data in the channel occupied by PUs. While for false alarm, the channel state is *idle* but the prediction channel state is *busy*. This will cause SUs to miss the spectrum opportunities. Thus, false alarm and miss detection will affect the actual service time of the SU and PU connections, respectively [24]. We denote the false alarm probability as P_{FA} and the miss detection probability as P_{MD} .

a) False Alarm

We change the notation of the actual service time of a SU connection from $X_j^{(k)}$ to $\hat{X}_j^{(k)}$ under the false alarm case, and can obtain [24]

$$E[\hat{X}_j^{(k)}] = \sum_{t=1}^{\infty} E[\hat{X}_j^{(k)} | X_j^{(k)} = t] Pr\{X_j^{(k)} = t\}. \quad (12)$$

where t means a SU connection with t slots and j is the priority of the SU connection.

In case of the false alarm, the idle channel cannot be used to transmit the SU data. We can regard it as the busy time and SU transmission is postponed to the next time slot. For

a SU connection with t time slots, if there are i slots with false alarm, the actual service time of this SU is extended to $(t+i)$ slots. Therefore, the conditional expectation of the service time in (12) follows the negative binomial distribution with parameter P_{FA} [24]. That is as in Eq. 13 (next page).

Substituting (13) into (12), we obtain $E[\hat{X}_j^{(k)}]$ as

$$\begin{aligned} E[\hat{X}_j^{(k)}] &= \sum_{t=1}^{\infty} \frac{t Pr\{X_j^{(k)} = t\}}{1 - P_{FA}} \\ &= \frac{E[X_j^{(k)}]}{1 - P_{FA}}. \end{aligned} \quad (14)$$

b) Miss Detection

When miss detection occurs, the PU connection will be impaired by the SU connections. This impaired data is required to be retransmitted in the next slot. Therefore, the actual service time of a PU connection will change from $X_p^{(k)}$ to $\hat{X}_p^{(k)}$. Similar to the false alarm case, we can obtain the expected service time of $\hat{X}_p^{(k)}$ as [24]

$$E[\hat{X}_p^{(k)}] = \sum_{t=1}^{\infty} E[\hat{X}_p^{(k)} | X_p^{(k)} = t] Pr\{X_p^{(k)} = t\}. \quad (15)$$

As with the case of false alarm, $\hat{X}_p^{(k)}$ in the miss detection also follows the negative binomial distribution with the miss detection probability P_{MD} . Thus we have Eq. 16 (next page). Substituting (16) into (15), we obtain $E[\hat{X}_p^{(k)}]$ as

$$\begin{aligned} E[\hat{X}_p^{(k)}] &= \sum_{t=1}^{\infty} \frac{t Pr\{X_p^{(k)} = t\}}{1 - P_{MD}} \\ &= \frac{E[X_p^{(k)}]}{1 - P_{MD}}. \end{aligned} \quad (17)$$

If we use $E[\hat{X}_j^{(k)}]$ ($E[\hat{X}_p^{(k)}]$) to replace $E[X_j^{(k)}]$ ($E[X_p^{(k)}]$) in the equations in Section IV-A, we can obtain the mathematical model of our spectrum handoff scheme for imperfect sensing (i.e., with false alarm and miss detection).

$$\begin{aligned}
E[\widehat{X}_j^{(k)} = t + i | X_j^{(k)} = t] &= \sum_{t=1}^{\infty} (t+i) \binom{t+i-1}{i} (1-P_{FA})^t (P_{FA})^i \\
&= \frac{t}{1-P_{FA}}
\end{aligned} \tag{13}$$

$$\begin{aligned}
E[\widehat{X}_p^{(k)} = t + i | X_p^{(k)} = t] &= \sum_{t=1}^{\infty} (t+i) \binom{t+i-1}{i} (1-P_{MD})^t (P_{MD})^i \\
&= \frac{t}{1-P_{MD}}.
\end{aligned} \tag{16}$$

V. QoE-DRIVEN SPECTRUM HANDOFF SCHEME

Existing queueing-based spectrum handoff schemes mainly consider the end-to-end delivery time of SU transmissions [5], [6], [9], [10]; they seldom consider the impact of other factors (such as PER, data rate, packet length, channel transmission rate and the signal-to-interference-noise-ratio (SINR)) on the end-user satisfaction. In this section, we describe a QoE-driven handoff scheme, which maximizes quality of the transmitted data while minimizing transmission delay. This handoff scheme simultaneously considers impact of the application and network level parameters, and spectrum handoff delay on the end-user satisfaction.

Traditionally, to maximize satisfaction of multimedia (e.g., video) users, we want to choose a channel which provides the highest possible peak signal-to-noise ratio (PSNR) of video transmission. Since estimating the video PSNR requires the decoding of video at the receiver, it is not feasible to use PSNR directly as the channel selection metric for spectrum handoff scheme. Therefore, we use a low-complexity substitute metric (i.e., mean opinion score (MOS)) to represent the effect of video PSNR. As a major QoE metric, MOS is widely used to evaluate the multimedia user's perception of quality [11]. The value of MOS is in the range of 1 to 5. In general, the higher the MOS, the higher is the PSNR.

In CRNs, SUs may experience different channel conditions over time even if they use the same channel. We consider two types of packet delivery failures: packet loss due to the delay caused by spectrum handoff, and packet error due to poor channel quality. We denote the PER of channel k for SU transmission with priority j as $PER_j^{(k)}$. For a given SINR, the PER can be approximated using a sigmoid function [19], [25] as

$$PER_j^{(k)} = \frac{1}{1 + e^{\eta(\text{SINR}_j^{(k)} - \sigma)}} \tag{18}$$

where η is the modulation and σ is the coding schemes. Both of them are constants for a given packet length.

Let $Delay_{j,i}$ be the delay of a SU connection with priority j due to the first $(i-1)$ interruptions. A SU packet with priority j will be dropped when its delay exceeds the delay deadline d_j . Let $PDR_{j,i}^{(k)}$ be the probability of packet being dropped during the i^{th} interruption. It equals to the probability of $E[D_{j,i}^{(k)}]$ being larger than $d_j - Delay_{j,i}$. By applying M/G/1

approximation in [4], [29], we can get $PDR_{j,i}^{(k)}$ as

$$PDR_{j,i}^{(k)} = \begin{cases} \rho_{j,i}^{(k)} \exp\left(-\frac{\rho_{j,i}^{(k)} \times (d_j - Delay_{j,i})}{E[D_{j,i}^{(k)}]}\right) & \text{if } \rho_{j,i}^{(k)} < 1 \\ 1 & \text{if } \rho_{j,i}^{(k)} \geq 1 \end{cases}, \tag{19}$$

where $\rho_{j,i}^{(k)}$ is the normalized load of channel k caused by type-(j,i) SU.

Let $TPER_{j,i}^{(k)}$ be the estimated total PER of channel k for the SU connection with priority j at its i^{th} interruption. Assuming channel PER and PDR are independent of each other, we have $TPER_{j,i}^{(k)} = PER_j^{(k)} + PDR_{j,i}^{(k)} - PER_j^{(k)} \cdot PDR_{j,i}^{(k)}$. Using the QoE model derived in [11], the expected MOS for a SU with priority j choosing channel k for its i^{th} interruption, $MOS_{j,i}^{(k)}$, can be represented as a function of the sender bitrate (SBR), frame rate (FR) and the $TPER_{j,i}^{(k)}$.

$$MOS_{j,i}^{(k)} = \frac{\tau_1 + \tau_2 FR + \tau_3 \ln(SBR)}{1 + \tau_4 (TPER_{j,i}^{(k)}) + \tau_5 (TPER_{j,i}^{(k)})^2}. \tag{20}$$

The coefficients $\tau_1, \tau_2, \tau_3, \tau_4, \tau_5$ can be obtained by a linear regression analysis [11]. In our handoff scheme, we focus on the analysis of MOS as a function of the expected spectrum handoff, while assuming other parameters of MOS including sender bitrate (SBR) and frame rate (FR) are fixed. Whenever a SU connection is interrupted, we choose the available channel with maximum expected MOS for spectrum handoff. In (20), maximizing the MOS does not simply mean minimizing the spectrum handoff delay. In order to maximize MOS, we need to choose a channel with the minimum estimated $TPER$, which depends on PER and PDR .

VI. A LEARNING-BASED QoE-DRIVEN SPECTRUM HANDOFF

We design an intelligent spectrum handoff scheme, in which each SU adaptively uses the evolutionary conditions to maximize its expected MOS. This can be achieved by modeling the spectrum handoff decisions as a Markov decision process (MDP) [30] with MOS metric as the action reward.

A (finite-state) MDP can be represented as a tuple (S, A, T, R) [30], where S denotes the set of system states; A is the set of candidate actions at each state; $T = \{P_{s,s'}(a)\}$ is the set of state transition probabilities, where $P_{s,s'}(a)$ is the state transition probability from state s to s' when taking

action a in state s ; and $R : S \times A \mapsto \mathfrak{R}$ specifies the reward (or cost) at $s \in S$ when taking action $a \in A$. An MDP model consists of the following iterative steps: 1) The agent senses the environment and observes $s \in S$. 2) Based on s , the agent chooses an action $a \in A$ to perform on the environment. 3) The environment makes a transition to a new state s' and generates a reward (or cost) $r \in R$. 4) The agent receives the reward and uses it to update the policy. 5) Repeat the process.

If the transition and reward models of MDP are known, we can use action iteration to obtain the optimal action for each SU. Its complexity is approximately n^2 , where n is the number of states. It is efficient when the state space is small. However, the probabilistic transition function is difficult to deduce in the distributed CRNs with complex and dynamic nature, where the state space is large. For a decentralized CRN, we can use distributed Q-learning [31], a model-free reinforcement learning (RL), to find optimal decision policies. It does not require the transition and reward models, and enables SUs to find an optimal policy $\pi^*(s) \in A$, i.e., a sequence of actions $\{a_1, a_2, a_3, \dots\}$ for s , to maximize the total expected discounted reward (or minimize the cost) in the long run. In the following sub-sections, we describe the distributed Q-learning for the QoE-driven spectrum handoff scheme.

1) *States of SU connections*: For a given SU_j connection, the network state before the $(i+1)^{th}$ interruption is denoted as $s_{j,i} = \{\xi_{j,i}^{(k)}, \omega_{j,i}^{(k)}, \phi_{j,i}^{(k)}\}$, where k is the channel at which SU_j is served when $(i+1)^{th}$ interruption occurs. $\xi_{j,i}^{(k)}$ represents the condition of channel k (e.g., physical PER). $\omega_{j,i}^{(k)}$ and $\phi_{j,i}^{(k)}$ represent the arrival rate and the service time, respectively, of type- (j,i) SU at channel k . The definitions and calculations of these state parameters were described in Sections IV-A and V.

2) *Actions of SU connections*: When a SU connection is interrupted, it needs to choose to stay at the current channel or switch to another available channel, as described in Section IV-A. We denote $a_{j,i} = \{\beta_{j,i}^{(k)}\} \in \mathcal{A}$ as the candidate actions of SU_j on state $s_{j,i}$ at its $(i+1)^{th}$ interruption. $\beta_{j,i}^{(k)}$ represents the channel selection parameter, which determines the probability of selecting channel k as the transmission channel after the $(i+1)^{th}$ interruption. When the expected spectrum handoff delay exceeds the delay deadline d_j , the packet will be dropped as described in Section V.

3) *Rewards of SU connections*: The reward r of an action is defined as the predicted MOS of multimedia transmission, for a certain handoff. The expected MOS in (20) is composed of two parts: the PER due to channel condition and the PDR when the expected delay of spectrum handoff exceeds the delay deadline. With this reward function, the Q-learning tries to maximize MOS while balancing the delay caused by spectrum handoff. From the description in Section IV, we can see that the expected delay of the video with higher priority will not be influenced by other SUs with lower priority. However, if the SU belongs to a lower priority class, the influence of the higher priority traffic is taken into account by the MOS metric, based on the priority-based queueing model.

4) *Online learning of SU connections*: The objective of the agent at the $(i+1)^{th}$ interruption is to find an optimal action which maximizes the expected MOS at current policy

$\pi^*(s_{j,i}, a_{j,i})$.

The Bellman optimality equation [31] takes into account the discounted long-term reward of taking an action. In order to make foresighted decision for the SU by considering the cumulative rewards over time, starting with state $s_{j,i}$, Bellman optimality equation is used as the utility function. The equation aims to find an optimal action, so that $\pi^*(s_{j,i}, a_{j,i})$ generates the maximum discounted accumulative rewards. To simplify the notation in the equations, we will use s to represent the state $s_{j,i}$ and s' to represent the new state $s_{j,i+1}$ after taking action $a_{j,i}$. Similarly, we use a to denote the action $a_{j,i}$ and a' to stand for the action $a_{j,i+1}$ on the new state $s_{j,i+1}$. We can denote Bellman optimality equation [31] of the MDP as:

$$\begin{aligned} V^*(s) &= \max_{a \in \mathcal{A}} E_{\pi^*} \left\{ \sum_{k=0}^{\infty} \gamma^k r_{j,i+k+1} \mid s_{j,i} = s, a_{j,i} = a \right\} \\ &= \max_{a \in \mathcal{A}} E_{\pi^*} \left\{ \sum_{k=0}^{\infty} \gamma^k MOS_{j,i+k+1}(a) \mid s_{j,i} = s, a_{j,i} = a \right\} \\ &= \max_{a \in \mathcal{A}} \left\{ E[MOS_{j,i+1}] + \gamma \sum_{s'} P_{s,s'}(a) V^*(s') \right\}, \end{aligned} \quad (21)$$

where $0 \leq \gamma \leq 1$ is a discount rate which decreases the utility impact of the later decisions. To ensure that the cumulative reward is bounded in the long run, γ should be less than 1 [31]. Setting $\gamma = 0$ makes the CRN node perform spectrum handoff in a myopic manner. This greedy method at each spectrum handoff process can reduce the future rewards, which would degrade the performance. As γ approaches to 1, the future rewards are taken into account more strongly in $V^*(s, a)$, which makes the agent become more farsighted. r is the reward of an action on a state, and is defined as the predicted MOS of multimedia transmission. $V^*(s, a)$ is the utility value for taking action $a = a_{j,i}$ at state $s = s_{j,i}$, and then executing the optimal policy π^* thereafter.

We can also express the Bellman optimality equation as the action-value function $Q^*(s, a)$

$$\begin{aligned} Q^*(s, a) &= E\{MOS_{j,i+1} + \gamma V^*(s') \mid s_{j,i} = s, a_{j,i} = a\} \\ &= E\{MOS_{j,i+1} + \gamma \max_{a' \in \mathcal{A}} Q^*(s', a') \mid s_{j,i} = s, a_{j,i} = a\} \\ &= E(MOS_{j,i+1}) + \gamma \sum_{s'} P_{s,s'}(a) \max_{a' \in \mathcal{A}} Q^*(s', a'). \end{aligned} \quad (22)$$

It is difficult to characterize the state transition probabilities due to the complex and dynamic nature of CRNs. Therefore, we use the model-free Q-learning which recursively updates the Q-values for a given connection during its multiple interruptions:

$$Q(s, a) = (1 - \alpha)Q(s, a) + \alpha \left\{ E(MOS_{j,i+1}) + \gamma \max_{a' \in \mathcal{A}} Q(s', a') \right\} \quad (23)$$

where $0 < \alpha < 1$ is the step-size parameter, which affects the rate of learning. Instead of using the ϵ -greedy policy [31] to select the action for exploration and exploitation, we use the soft-max policy [31] for action selection. Assuming $\pi(s, a)$ denotes the probability of an agent taking the action a given the state s at its $(i+1)^{th}$ interruption, the softmax

Algorithm 1 The learning-based QoE-driven handoff scheme.

```

Input:  $\lambda_j^{(k)}, E[X_j^{(k)}], \forall j, \forall k, \nu, \gamma$ 
Output: The best policy  $\pi(s, a)$ 
1) Initialize  $Q(s, a)$  arbitrarily.
2) Generate PUs' and SUs' arriving time by using  $\lambda_j^{(k)}$ .
3) Repeat (for each episode):
4) Initialize all states  $s$ .
5) Repeat (for each step of episode):
6) if  $PU_j$  arrives at channel  $k$ 
7) if channel  $k$  is idle
8)  $PU_j$  is served at channel  $k$ .
9) elseif channel  $k$  is occupied by other PU
10)  $PU_j$  enters into queue  $Q_p^{(k)}$ .
11) elseif channel  $k$  is occupied by  $SU_j$ 
12)  $SU_j$  is interrupted and performs spectrum handoff
13) Choose action  $a$  for  $s$  using policy derived from  $Q$ .
14) Perform spectrum handoff according to action  $\alpha$ .
15) if the switching channel == current channel
16) Calculate the waiting time  $E[W_j^{(k)}]$  using (2).
17) //The total delay  $Delay_{j,i}$  of the first  $i^{th}$  interruptions.
18)  $Delay_{j,i+1} = Delay_{j,i} + E[W_j^{(k)}]$ .
19) if  $Delay_{j,i+1} >= SU_j$  delay deadline
20) Drop the packet and repeat the process.
21) end if
22) //New arriving PU will use this channel
23)  $SU_j$  is pushed into the head of queue  $Q_j^{(k)}$ .
24) elseif
25) Calculate the waiting time  $E[W_j^{(k)}]$  using (3).
26) //The total delay  $Delay_{j,i}$  of the first  $i^{th}$  interruptions.
27)  $Delay_{j,i+1} = Delay_{j,i} + E[W_j^{(k)}]$ .
28) if  $Delay_{j,i+1} >= SU_j$  delay deadline
29) Drop the packet and repeat the process.
30) end if
31) if the switching channel  $k'$  is serving other SU
32)  $SU_j$  is pushed into the tail of queue  $Q_j^{(k')}$ .
33) else
34)  $SU_j$  is being served at channel  $k'$ .
35) end if
36) end if
37) Calculate the PDR using (19).
38) Calculate the expected MOS using (20).
39) //Update the Q-values
40)  $Q(s, a) \leftarrow (1 - \alpha)Q(s, a) + \alpha\{E(MOS_{j,i+1}) + \gamma \max_{a' \in \mathcal{A}} Q(s', a')\}$ .
41)  $s \leftarrow s'$ .
42) Update the policy  $\pi(s, a)$  using (24).
43)  $PU_j$  is being served at channel  $k$ .
44) end if
45) elseif new SU arrives at channel  $k$ 
46) if channel  $k$  has higher priority SUs waiting in queue
47) Dequeue and serve the SU with the highest priority.
48) New arriving SU enters the queue.
49) else
50) New arriving SU is being served.
51) end if
52) else
53) Dequeue and serve the SU with the highest priority.
54) end if
55) until  $s$  is terminal

```

policy is defined using the Boltzmann distribution [31], [32]:

$$\pi(s, a) = \frac{\exp(\frac{Q(s,a)}{v})}{\sum_{a_m \in \mathcal{A}} \exp(\frac{Q(s,a_m)}{v})} \quad (24)$$

where parameter v is a positive value called as the temperature. The high temperatures cause the actions to be nearly equiprobable whereas the low temperatures cause a greater difference in selection probabilities for actions that differ in

their Q value estimates [31]. As $v \rightarrow 0$, softmax action selection becomes the same as the greedy action selection. The model-free distributed Q-learning can achieve the maximum rewards in the long term, and is guaranteed to converge to the optimal value [31].

The system diagram of the proposed spectrum handoff scheme is shown in Fig. 3. The CRN node first observes the current state $s_{j,i}$ of SU_j connection at its i^{th} interruption. After being interrupted again by a PU, the CRN node selects a handoff action for $(i+1)^{th}$ interruption of SU_j connection according to the current state from Q-learning engine. Then, SU_j connection performs spectrum handoff and transits to a new state $s_{j,i+1}$. After transition, CRN node obtains a reward and updates the Q-table for state $s_{j,i}$.

The proposed scheme is discussed in Algorithm 1.

VII. EXPERIMENTAL RESULTS

In this section, we evaluate the performance of our spectrum handoff scheme. In the proposed mixed queueing model in Section III, we assumed that the service time of PUs and SUs follows a general distribution. In our experiments, we assume that the service time of PUs and SUs have the exponential distribution, for mathematical tractability, which is also a widely-used distribution in CRNs. For exponential distribution, the service time $E[X] = \frac{1}{\mu}$ and the remaining transmission time of SUs still follows the same exponential distribution after being interrupted by PUs [7]. Therefore, the interruption probability of SUs is independent of the number of interruptions. Referring to [7], we have the arrival rate of a type- (j, i) SU connection at channel k as $\omega_{j,i}^{(k)} = \lambda_j^{(k)} (\frac{\lambda_p^{(k)}}{\lambda_p^{(k)} + \mu_j^{(k)}})^i$, and the effective service time as $E[\Phi_{j,i}^{(k)}] = \frac{1}{\lambda_p^{(k)} + \mu_j^{(k)}}$.

In the experiments, the time slot duration of 10 msec is used, as recommended by the IEEE 802.22 standard [21].

A. QoS-aware Spectrum Handoff Scheme

In this section, we study the average SU delivery time and the average number of spectrum interruptions, using a delay-driven spectrum handoff scheme that aims to reduce the delivery time of SU connections [6]. We also compare the performance of our proposed mixed priority queueing model with two recently developed queueing models in [4] and [6]. The number of channels is $M = 3$, and the number of priority classes of SU connections is $N = 4$, such that class j has a higher priority than $j + 1$.

1) *Effect of the PU Traffic Load:* We assume that all SU connections have the same arrival rate and expected service time. To simplify the notation, we denote $\lambda_j^{(k)}$ as λ_j , and $E[X_j^{(k)}]$ as $E[X_j]$, for all channel numbers k , ($1 \leq k \leq M$) and priority classes j , ($1 \leq j \leq N$).

In Fig. 4(a), average data delivery time of all SU connections with different priorities increases with normalized PU traffic load. Our proposed queueing model has better performance than the model in [4] for all SU connections regardless of their priorities. This is because a SU connection (in [4]) stays at its current channel whenever interrupted, instead of using better channels. Also, higher-priority SU connections can interrupt the lower-priority SU connections,

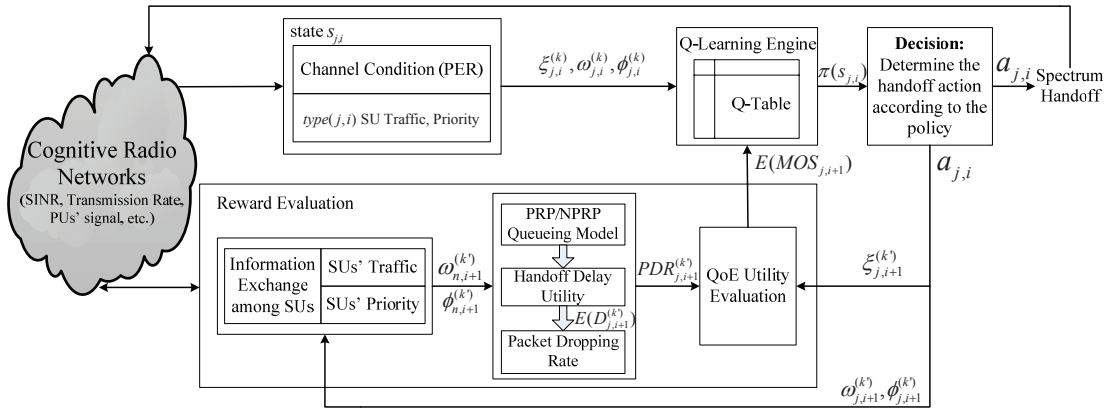


Fig. 3. The system diagram of the proposed learning-based QoE-driven spectrum handoff scheme.

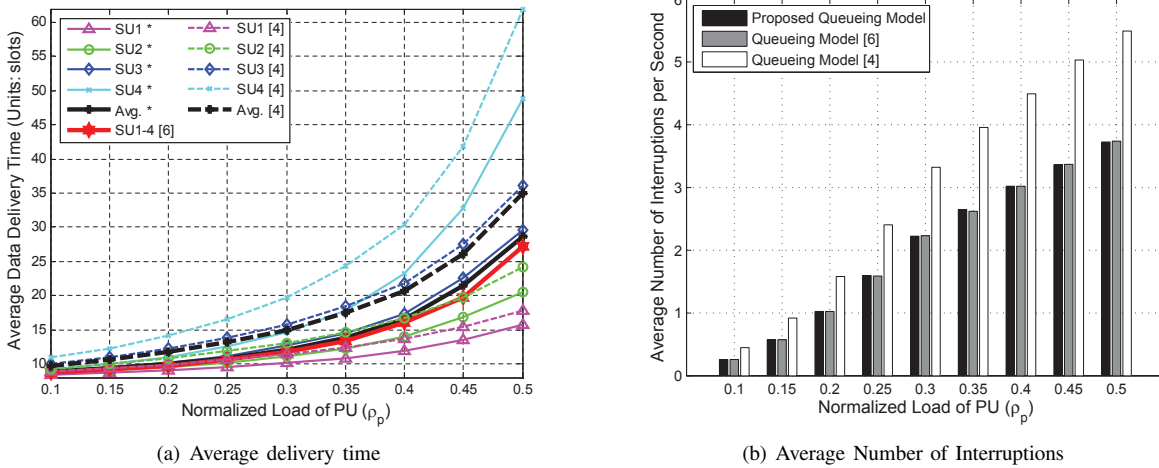


Fig. 4. Effects of the normalized PU traffic load (ρ_p) on the average delivery time and the average number of interruptions per second for $E[X_p] = 10(\text{slots/arrival})$, $\lambda_s = 0.03(\text{arrivals/slot})$, and $E[X_s] = 8(\text{slots/arrival})$. The symbol "*" in the legend denotes our proposed queueing model.

which causes frequent spectrum handoffs, resulting in larger transmission delay in [4]. The higher-priority SU connections have lower average delivery time in our queueing scheme, than those using the queueing model in [6], because our queueing model allocates more channel resources to them. Our overall average delivery time is comparable to the model in [6], but much lower than the model in [4].

For conciseness, we only show the average number of interruptions in Fig. 4(b). The queueing model in [4] has more interruptions than our model, because the arriving SUs with higher priorities interrupt the ongoing lower-priority SU connections in [4], which causes the frequent spectrum interruptions. The average number of interruptions in [6] is almost the same as our scheme. However, the higher-priority SU connections have lower number of interruptions in our scheme than in [6], which is not shown in Fig. 4(b).

2) *Effect of the SU Traffic Load:* In this set of experiments, we evaluate the performance, in terms of average SU delivery time and average number of spectrum interruptions, for different SU traffic loads. In the experiment, the SU connections with different priorities have the same service time, and the PU connections in different channels have the same settings with $\lambda_p^{(k)} = \lambda_p = 0.05(\text{arrivals/slot})$ and $E[X_p^{(k)}] = E[X_p] = 6(\text{slots/arrival})$.

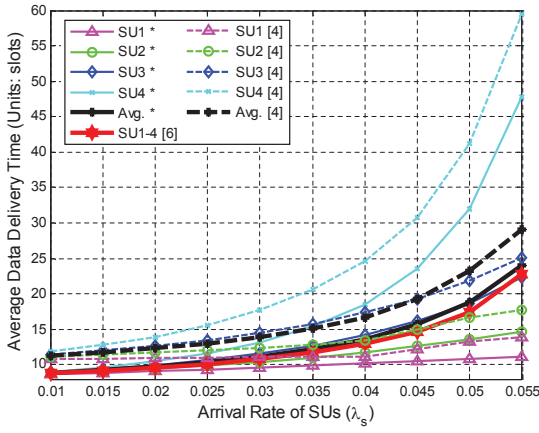
Fig. 5(a) shows the average data delivery time of the SU

connections for different SU arrival rates. We conclude that: 1) the average delivery time of SU connections increases with SU arrival rate because more SU connections need to access the channel at the same time, resulting in longer waiting time. 2) For the same SU traffic load, the delivery time of higher-priority SU connections is lower in our queueing model than the model in [6], where all SUs have the same priority. However, our queueing model has comparable overall average delivery time. 3) The delivery time of all SU connections in our queueing model is lower than in [4]. The reasons are similar to those discussed in Section VII-A1.

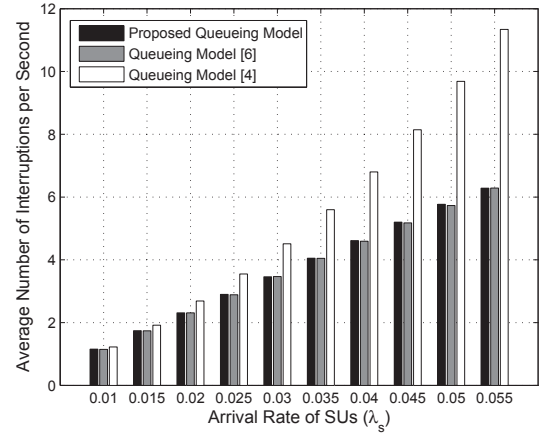
In Fig. 5(b), using the queueing model in [4] has higher number of interruptions than using our proposed queueing model. Also, the average number of interruptions increases with the arrival rate of SUs.

B. QoE-driven Spectrum Handoff Scheme

In this section, we evaluate the performance of our QoE-driven spectrum handoff scheme based on our mixed PRP/NRP M/G/1 queueing model, for transmission of two CIF videos, Bus and Foreman. These sequences were encoded using H.264/AVC JM reference software [33] for a GOP length of 30 frames at 30 frames/sec. The FR (30 frames/sec) and SBR (200Kbps) are fixed. The number of channels is



(a) Average Delivery Time



(b) Average Number of Interruptions

Fig. 5. The effects of SU arrival rate on the average delivery time and the average number of interruptions per second for $\lambda_p=0.05$ (arrivals/slot), $E[X_p]=6$ (slots/arrival) and $E[X_s] = 8$ (slots/arrival). The symbol '*' in the legend denotes our proposed queueing model.

TABLE II
THE PACKET ERROR RATES.

SU	CH1	CH2	CH3	CH4	d_j (sec)
SU1	16%	3%	2%	17%	0.5
SU2	8%	19%	18%	3%	0.5
SU3	17%	4%	15%	3%	0.5
SU4	16%	4%	3%	14%	0.5
SU5	3%	16%	18%	5%	0.5
SU6	3%	14%	4%	17%	0.5

TABLE III
COMPARISONS OF TPER VALUES FOR DIFFERENT NORMALIZED LOADS OF PU (ρ_p).

	ρ_p							
		0.1	0.2	0.3	0.4	0.5	0.6	0.7
SU1	Delay	10.50%	11.35%	11.90%	13.52%	15.63%	17.52%	20.40%
	QoE	3.88%	5.26%	6.97%	9.43%	12.50%	15.03%	18.59%
SU2	Delay	13.40%	14.97%	16.51%	19.13%	22.07%	26.36%	31.08%
	QoE	6.91%	7.96%	10.65%	13.90%	17.96%	23.20%	27.54%
SU3	Delay	12.40%	14.93%	18.08%	21.43%	27.22%	31.29%	37.95%
	QoE	7.57%	10.46%	14.06%	18.66%	24.05%	29.13%	34.00%
SU4	Delay	14.24%	17.37%	21.67%	27.86%	34.20%	39.59%	46.97%
	QoE	9.48%	14.04%	19.19%	25.05%	31.77%	36.96%	43.29%
SU5	Delay	17.11%	21.39%	28.30%	34.74%	42.33%	48.57%	55.56%
	QoE	11.29%	15.62%	22.84%	28.56%	37.33%	43.94%	51.26%
SU6	Delay	19.26%	25.05%	32.82%	40.03%	48.63%	56.04%	61.17%
	QoE	14.13%	20.08%	28.43%	35.95%	44.11%	52.11%	57.25%

Note: $\lambda_s = 0.05$ (arrivals/slot), $E[X_s] = 10$ (slots/arrival), and $E[X_p] = 20$ (slots/arrival).

$M = 4$ and the number of priority classes of SU connections is $N = 6$, where class j has higher priority than class $j + 1$.

For generality, we assume that different SUs experience different channel conditions on any given channel as in [4], [19]. For instance, the PER of each channel for each SU in Table II is different and does not depend on its priority.

Tables III and IV show the TPER for different normalized loads of PU and different arrival rates of SUs, respectively, for the delay-driven (Delay) and the QoE-driven spectrum handoff scheme (QoE). The QoE-driven spectrum handoff scheme has a lower TPER by 3% ~ 6% than the delay-driven scheme. The results are expected, since the delay-driven scheme does not consider the effect of channel errors, whereas the QoE-

TABLE IV
COMPARISONS OF TPER VALUES FOR DIFFERENT ARRIVAL RATES OF SU CONNECTIONS (λ_s ((ARRIVALS/SLOT))).

	λ_s							
		0.01	0.015	0.02	0.025	0.03	0.035	0.04
SU1	Delay	11.13%	11.70%	12.18%	12.26%	12.68%	13.01%	13.16%
	QoE	5.76%	6.65%	6.86%	7.69%	7.78%	8.42%	8.63%
SU2	Delay	13.36%	14.14%	14.97%	15.96%	16.40%	16.50%	17.72%
	QoE	9.28%	10.43%	10.06%	10.94%	11.10%	12.18%	12.60%
SU3	Delay	11.36%	12.43%	13.66%	14.49%	16.00%	18.15%	19.36%
	QoE	7.12%	8.11%	9.25%	10.41%	12.63%	12.90%	15.93%
SU4	Delay	11.14%	12.27%	13.69%	15.57%	18.13%	20.08%	23.19%
	QoE	7.46%	8.30%	9.62%	12.16%	14.36%	16.81%	20.18%
SU5	Delay	12.55%	13.91%	15.81%	18.40%	21.18%	24.32%	28.13%
	QoE	8.63%	9.75%	11.12%	13.84%	16.76%	18.94%	22.87%
SU6	Delay	11.91%	13.65%	16.18%	19.53%	23.25%	26.37%	31.26%
	QoE	7.41%	8.68%	11.09%	13.85%	18.06%	23.11%	27.17%

Note: $\lambda_p = 0.02$ (arrivals/slot), $E[X_p] = 20$ (slots/arrival), and $E[X_s] = 10$ (slots/arrival).

driven scheme considers both transmission delay and channel errors when choosing the target channel.

Figs. 6 and 7 show the resulting MOS and PSNR of Foreman videos, corresponding to the TPER results in Table III and Table IV. For conciseness, we only show the MOS and PSNR results of SU connection with priority 1, 2 and 4 in the figure. Our QoE-driven spectrum handoff scheme achieves obvious improvement in average MOS and video PSNR over the delay-driven spectrum handoff scheme. We also get similar improvements for Bus video sequence.

C. Performance under Heterogeneous Service Requirements

In this experiment, we study the performance of our QoE-driven spectrum handoff scheme for SU connections with different delay requirements. Here, the number of channels is $M = 3$ and number of priority classes of SU connections is $N = 4$. The PER of channel 1, channel 2, and channel 3 are 2%, 6%, and 10%, respectively. The delay deadline for SU_1 , SU_2 , SU_3 , and SU_4 are 0.5sec, 1sec, 3sec, and no delay deadline, respectively. Since SU_1 has the most strict delay constraint (such as in video conferencing), we assign

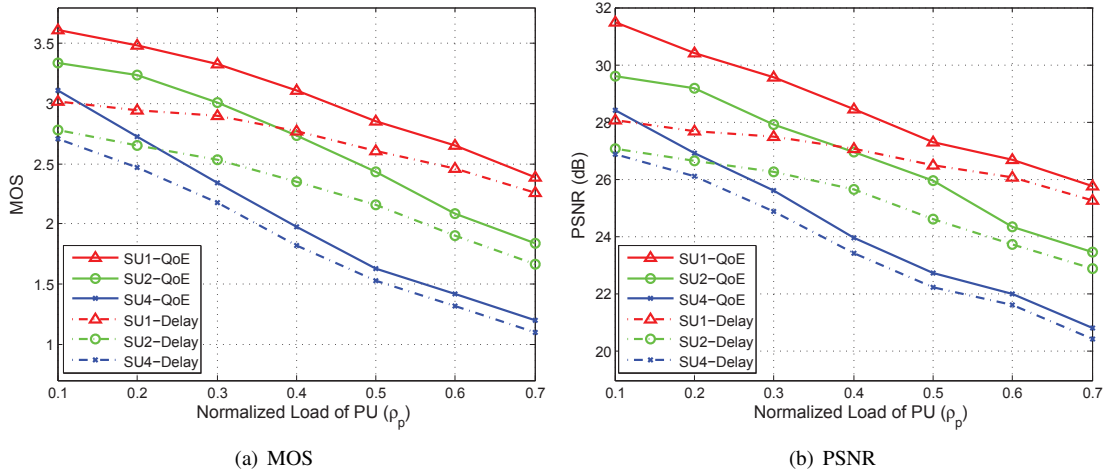


Fig. 6. MOS and average PSNR of Foreman video sequence vs. the normalized load of PU (ρ_p) for $\lambda_s = 0.05$ (arrivals/slot), $E[X_s] = 10$ (slots/arrival), and $E[X_p] = 20$ (slots/arrival). The lossless PSNR of Foreman sequence is 36.81dB.

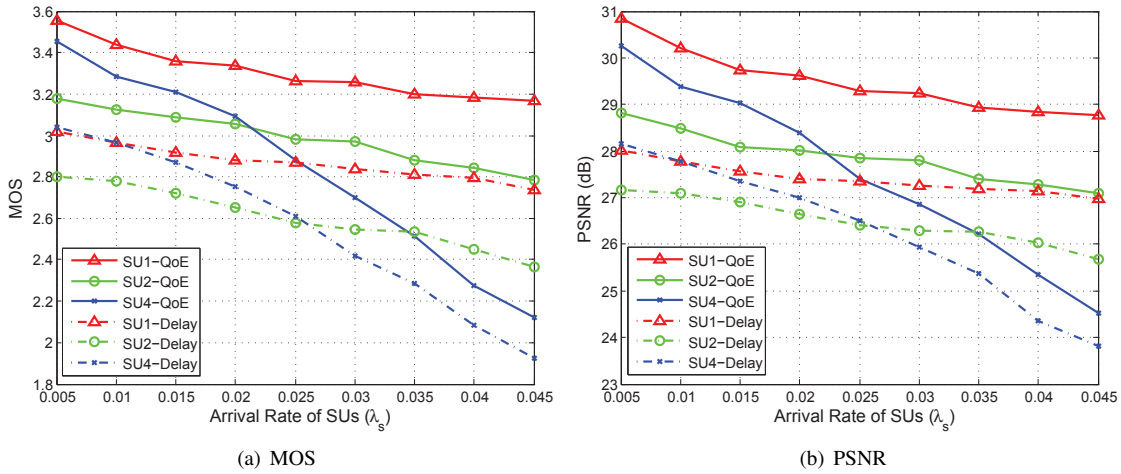


Fig. 7. MOS and average PSNR of Foreman video sequence vs. the arrival rate of SUs (λ_s) for $\lambda_p = 0.02$ (arrivals/slot), $E[X_p] = 20$ (slots/arrival), and $E[X_s] = 10$ (slots/arrival). The lossless PSNR of Foreman sequence is 36.81dB.

the highest priority to it. The delay deadlines of SU_2 and SU_3 are suitable for streaming applications. SU_4 can represent the FTP or other non-real-time data application as it does not have a delay deadline.

In Fig. 8, SU_3 has lower $TPER$ than SU_1 and SU_2 for $\lambda_s \leq 0.03$ because it has a larger delay deadline, and, therefore, less packets are dropped during spectrum handoff when the arrival rate of SUs is lower. For the same reason, SU_2 has a lower $TPER$ than SU_1 for $\lambda_s \leq 0.04$. However, the $TPER$ of SU_3 increases quickly when the SU arrival rate $\lambda_s \geq 0.035$, because many packets of SU_3 , which has a lower priority, are dropped as they expire during the handoff and also due to the higher channel PER. On the other hand, the $TPER$ of SU_1 increases slowly with λ_s because it has the highest priority and our QoE-based queueing model selects a channel with the maximum MOS for it. Also, the $TPER$ of SU_4 is always very low because its packets are not dropped due to the delay deadline.

D. RL-enhanced QoE-driven Spectrum Handoff Scheme

In this section, we evaluate the performance of our learning-based QoE-driven spectrum handoff scheme based on the

TABLE V
SIMULATION PARAMETERS IN TERMS OF PER.

SU	CH1	CH2	CH3	d_j (sec)
SU1	16%	3%	11%	0.5
SU2	2%	18%	10%	0.5
SU3	17%	9%	4%	0.5
SU4	10%	16%	4%	0.5

mixed PRP/NPRP M/G/1 queueing model. The video parameters are set to the same value as described in Section VII-B. The number of channels is $M = 3$ and the number of priority classes of SU connections is $N = 4$. The PER of each channel for each SU is shown in Table V.

The discount rate (γ) of our RL-based QoE-driven spectrum handoff scheme is set to be 0.5. For myopic QoE-driven spectrum handoff scheme, we set $\gamma = 0$. The temperature v in the softmax policy is set to be 0.4. We choose the channel for handoff according to the procedure described in Section VI for each interruption.

Fig. 9 shows the expected MOS value for learning-based and myopic handoff schemes for different traffic loads. The learning-based handoff scheme outperforms myopic handoff scheme for different PU and SU traffic loads because the agent

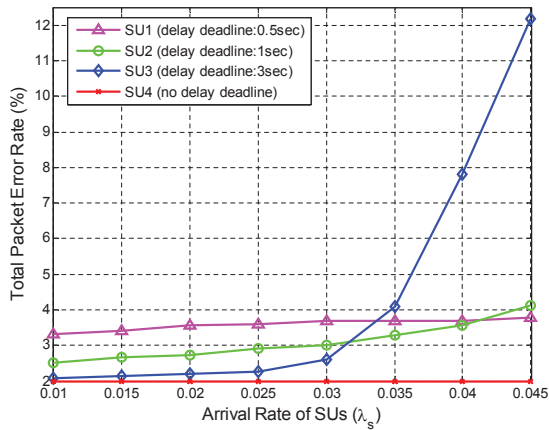


Fig. 8. Total Packet Error Rate (TPER) of the SU connection with different delay deadlines vs. the arrival rate of SUs (λ_s) for $\lambda_p = 0.05$ (arrivals/slot), $E[X_p] = 6$ (slots/arrival), and $E[X_s] = 8$ (slots/arrival).

in our handoff scheme considers the effect of the current action on the future rewards to maximize the expected MOS in long run.

In Fig. 9(a) and Fig. 9(b), the expected MOS decreases when the arrival rate (λ_p) of PU connection increases because it causes more interruptions for SU connections. This also forces the SU connections to wait for longer time to be served which leads to their expiry. Similarly, the expected MOS decreases when the arrival rate (λ_s) of SU connection increases in Fig. 9(a) and Fig. 9(c). In Fig. 9(a) and Fig. 9(d), the expected MOS decreases when the service time ($E[X_s]$) of an SU connection increases, because the SU with a longer service time is more likely to be interrupted by PUs. Thus, the SU connection needs to spend more time to find a channel for handoff.

In Fig. 10, we compare the visual result of the RL-based and myopic QoE-driven spectrum handoff schemes for SU1. These video results match with the result of Fig. 9(a).

VIII. CONCLUSIONS

In this paper, we proposed a mixed PRP/NRP M/G/1 queueing model to manage the spectrum usage behavior for multimedia applications in CRNs. The queueing model is designed to meet the prioritized transmission requirements while avoiding the excessive delay caused by frequent spectrum handoffs. The mathematical analysis of the SU delay performance shows that our proposed spectrum handoff scheme can optimize utility functions related to SU delay performance. Based on the queueing model and its analysis framework, a QoE-driven spectrum handoff scheme was proposed to meet the end-user satisfaction of heterogeneous multimedia users. Experimental results show that our proposed mixed priority queueing model can achieve better delay performance than other recently-developed queueing models. The proposed QoE-driven spectrum handoff scheme with the mixed queueing model improves the end-user satisfaction in terms of both delivery time and video PSNR compared to the delay-driven spectrum handoff scheme.

REFERENCES

- [1] Federal Communications Commission, "Spectrum Policy Task Force Report," in *Et docket no. 02-135*, Nov. 2002.
- [2] J. Mitola and G. Q. Maguire, "Cognitive Radio: Making Software Radios More Personal," in *IEEE Personal Commun.*, vol. 6, 1999, pp. 13–18.
- [3] I. Christian, M. Sangman, I. Chung, and J. Lee, "Spectrum Mobility in Cognitive Radio Networks," in *IEEE Commun. Mag.*, vol. 50, Jun. 2012, pp. 114–121.
- [4] H.-P. Shiang and M. van der Schaar, "Queuing-Based Dynamic Channel Selection for Heterogeneous Multimedia Applications over Cognitive Radio Networks," in *IEEE Trans. Multimedia*, vol. 10, Aug. 2008, pp. 896–909.
- [5] L. Zhang, T. Song, M. Wu, J. Guo, D. Sun, and B. Gu, "Modeling for Spectrum Handoff Based on Secondary Users with Different Priorities in Cognitive Radio Networks," in *Int. Conf. on Wireless Commun. & Signal Proc. (WCSP)*, Oct. 2012, pp. 1–6.
- [6] L.-C. Wang, C.-W. Wang, and C.-J. Chang, "Modeling and Analysis for Spectrum Handoffs in Cognitive Radio Networks," in *IEEE Trans. Mobile Computing*, vol. 11, Sept. 2012, pp. 1499–1513.
- [7] C.-W. Wang and L.-C. Wang, "Modeling and Analysis for Proactive Decision Spectrum Handoff in Cognitive Radio Networks," in *Proc. IEEE ICC*, Jun. 2009, pp. 1–6.
- [8] C. Zhang, X. Wang, and J. Li, "Cooperative Cognitive Radio with Priority Queuing Analysis," in *Proc. IEEE ICC*, Jun. 2009.
- [9] S. Yoon and E. Ekici, "Voluntary Spectrum Handoff: A Novel Approach to Spectrum Management in CRNs," in *Proc. IEEE ICC*, May 2010, pp. 1–5.
- [10] Y. Song and J. Xie, "ProSpect: A Proactive Spectrum Handoff Framework for Cognitive Radio Ad Hoc Networks without Common Control Channel," in *IEEE Trans. Mobile Computing*, vol. 11, Jul. 2012, pp. 1127–1139.
- [11] A. Khan, L. Sun, E. Jammeh, and E. Ifeakor, "Quality of Experience-Driven Adaptation Scheme for Video Applications over Wireless Networks," in *IET Communications*, vol. 4, Jul. 2010, pp. 1337–1347.
- [12] Y. Wu, F. Hu, S. Kumar, M. Guo, and K. Bao, "Spectrum Handoffs with Mixed-Priority Queueing Model over Cognitive Radio Networks," in *IEEE GlobalSIP*, Dec. 2013.
- [13] Y. Li, S. Jayaweera, M. Bkassiny, and K. Avery, "Optimal Myopic Sensing and Dynamic Spectrum Access in Centralized Secondary Cognitive Radio Networks with Low-Complexity Implementations," in *Proc. IEEE VTC*, May. 2011, pp. 1–5.
- [14] Y. Song and J. Xie, "Performance Analysis of Spectrum Handoff for Cognitive Radio Ad Hoc Networks Without Common Control Channel under Homogeneous Primary Traffic," in *Proc. IEEE INFOCOM*, Apr. 2011, pp. 3011–3019.
- [15] S. Zheng, X. Yang, S. Chen, and C. Lou, "Target Channel Sequence Selection Scheme for Proactive-Decision Spectrum Handoff," in *IEEE Commun. Lett.*, vol. 15, Dec. 2011, pp. 1332–1334.
- [16] Y. Zhang, "Spectrum Handoff in Cognitive Radio Networks: Opportunistic and Negotiated Situations," in *Proc. IEEE ICC*, Jun. 2009.
- [17] L. Giupponi and A. Perez-Neira, "Fuzzy-based Spectrum Handoff in Cognitive Radio Networks," in *Int. Conf. on Cognitive Radio Oriented Wireless Netw. and Commun.*, May 2008, pp. 1–6.
- [18] M. NoroozOliaee, B. Hamdaoui, X. Cheng, T. Znati, and M. Guizani, "Analyzing Cognitive Network Access Efficiency under Limited Spectrum Handoff Agility," in *IEEE Trans. Veh. Technol.*, vol. 63, Mar. 2014, pp. 1402–1407.
- [19] H.-P. Shiang and M. van der Schaar, "Online Learning in Autonomic Multi-hop Wireless Networks for Transmitting Mission-Critical Applications," in *IEEE J. Sel. Areas Commun.*, vol. 28, Jun. 2010, pp. 728–741.
- [20] H. Su and X. Zhang, "Cross-Layer Based Opportunistic MAC Protocols for QoS Provisionings over Cognitive Radio Wireless Networks," in *IEEE J. Sel. Areas Commun.*, vol. 26, Jan. 2008, pp. 118–129.
- [21] IEEE Std 802.22-2011, Wireless Regional Area Network (WRAN) Specific Requirements Part 22: Cognitive Wireless RAN Medium Access Control (MAC) and Physical Layer (PHY) Specifications: Policies and Procedures for Operation in the TV Bands, in *IEEE*, Jul. 2011.
- [22] J. Wang, H. Zhai, and Y. Fang, "Opportunistic Packet Scheduling and Media Access Control for Wireless LANs and Multi-hop Ad Hoc Networks," in *IEEE Wireless Commun. Netw. Conf.*, vol. 2, Mar. 2004, pp. 1234–1239.
- [23] D. Bertsekas and R. Gallager, *Data Networks*. Upper Saddle River, NJ: Prentice Hall Inc., 1987.
- [24] L.-C. Wang, C.-W. Wang, and F. Adachi, "Load-Balancing Spectrum Decision for Cognitive Radio Networks," in *IEEE J. Sel. Areas Commun.*, vol. 29, Apr. 2011, pp. 757–769.

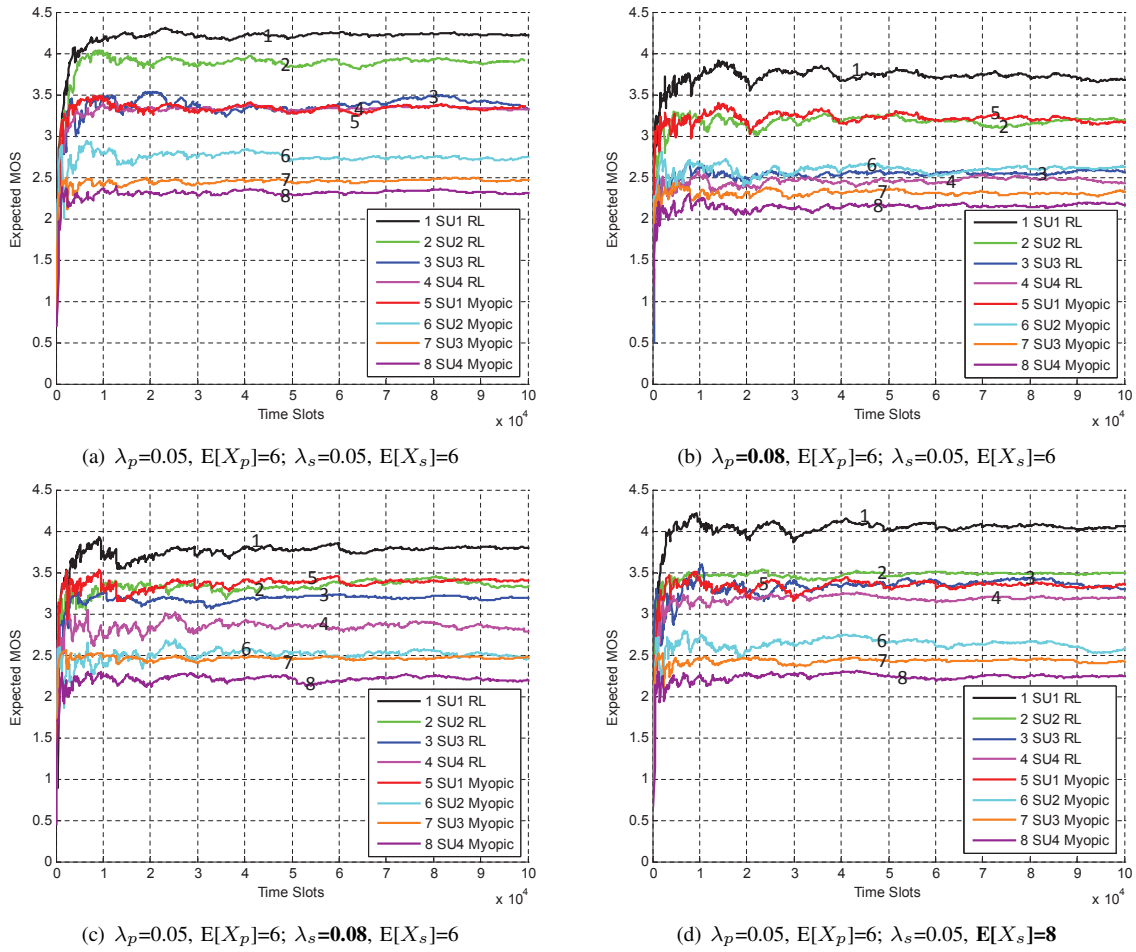


Fig. 9. The expected MOS for different PUs and SUs traffic loads.



Fig. 10. Visual comparison (Frame 31) of RL-based and Myopic-based QoE-driven spectrum handoff schemes for Bus sequence for SU1, where $\lambda_p = 0.05$ (arrivals/slot), $E[X_p] = 6$ (slots/arrival), $\lambda_p = 0.05$ (arrivals/slot), and $E[X_s] = 6$ (slots/arrival).

[25] D. Krishnaswamy, "Network-assisted link adaptation with power control and channel reassignment in wireless networks," in *3G Wireless Conf.*, 2002, pp. 165–170.

[26] X.-L. Huang, G. Wang, and F. Hu, "Multitask Spectrum Sensing in Cognitive Radio Networks via Spatiotemporal Data Mining," in *IEEE Trans. Veh. Technol.*, vol. 62, Feb. 2013, pp. 809–823.

[27] X.-L. Huang, G. Wang, F. Hu, and S. Kumar, "The Impact of Spectrum Sensing Frequency and Packet-Loading Scheme on Multimedia Transmission over Cognitive Radio Networks," in *IEEE Trans. Multimedia*, vol. 13, Jul. 2011, pp. 748–761.

[28] M. Guo, F. Hu, Y. Wu, S. Kumar, and J. D. Matyjas, "Feature-based Compressive Signal Processing (CSP) Measurement Design for the Pattern Analysis of Cognitive Radio Spectrum," in *Proc. IEEE GLOBECOM*, Dec. 2013.

[29] T. Jiang, C. K. Tham, and C. C. Ko, "An Approximation for Waiting Time Tail Probabilities in Multiclass Systems," in *IEEE Commun. Lett.*, vol. 5, Apr. 2001, pp. 175–177.

[30] M. L. Puterman, *Markov Decision Process: Discrete Stochastic Dynamic Programming*. John Wiley & Sons, Inc. New York, 1994.

[31] R. S. Sutton and A. G. Barto, *Reinforcement Learning: An Introduction*. Cambridge, MA: MIT press, 1998.

[32] C. J. C. H. Watkins and P. Dayan, "Q-learning," in *Machine Learning*, vol. 8, May 1992, pp. 279–292.

[33] JVT, H.264/AVC reference software JM14.2, ISO/IEC Std. [Online]. Available: <http://iphome.hhi.de/suehring/tml/download/>.



Yeqing Wu received his M.S. degree from the Department of Electronic Engineering, Shanghai Jiao Tong University, Shanghai, China, in 2008 and B.S. degree from the Department of Electronic Engineering, Tongji University, Shanghai, China, in 2002. He is currently pursuing his Ph.D. in the Department of Electrical and Computer Engineering at the University of Alabama, Tuscaloosa, USA. His research interests include cognitive radio networks, machine learning, rateless codes, and multimedia transmissions.



Yingying Zhu received her B.S. degree in Engineering in 2004 from Shanghai Maritime University. She received her M.S. degrees in Engineering in 2007 and 2010 from Shanghai Jiao Tong University and Washington State University, respectively. She is currently pursuing her Ph.D. in Intelligent Systems in the Department of Electrical Engineering at the University of California, Riverside. Her main research interests include computer vision, pattern recognition and machine learning, image/video processing and communication.



Fei Hu is an associate professor in the Department of Electrical and Computer Engineering at the University of Alabama (main campus), Tuscaloosa, Alabama, USA. He obtained his Ph.D. degrees at Tongji University (Shanghai, China) (in 1999), and at Clarkson University (New York, USA) in Electrical and Computer Engineering (in 2002). He has published over 160 journal/conference papers and books. Dr. Hu's research has been supported by U.S. National Science Foundation, U.S. Air Force Research Laboratory, Cisco, Sprint, and other sources.

His research interests are 3S - Security, Signals, and Sensors, including the cyber attacks in complex wireless or wired networks, cyber-physical system security and medical security issues, machine learning algorithms to process sensing signals in a smart way in order to extract patterns, micro-sensor design and wireless sensor networking issues.



Ali Talari received his MS degree in electrical engineering from Sharif University of Technology, Tehran, Iran, in 2006. He received his PhD in the School of Electrical and Computer Engineering at Oklahoma State University in 2012. His research interests are in novel error control coding techniques, communications theory, signal processing in wireless sensor networks, and compressive sensing techniques.



Nazanin Rahnavard received her B.S. and M.S. degrees in electrical engineering from the Sharif University of Technology, Tehran, Iran, in 1999 and 2001, respectively. She then received her Ph.D. in the School of Electrical and Computer Engineering at the Georgia Institute of Technology, Atlanta, in 2007. She is currently an Associate Professor in the Department of Electrical Engineering and Computer Science at the University of Central Florida, Orlando, FL. Dr. Rahnavard is the recipient of NSF CAREER award in 2011. She also received the 2007

Outstanding Research Award from the Center of Signal and Image Processing at Georgia Tech. She has interest and expertise in a variety of research topics in the communications, networking, and signal processing areas. She serves on the editorial board of the Elsevier Journal on Computer Networks (COMNET) and on the Technical Program Committee of several prestigious international conferences.



Sunil Kumar received his Ph.D. from the Birla Institute of Technology and Science, Pilani (India) in 1997. Currently, he is a Professor and Thomas G. Pine Faculty Fellow in the Electrical and Computer Engineering department at San Diego State University, CA. His research interests include robust video compression (including H.264 and HEVC), and QoS-aware and cross-layer protocols for wireless networks. He has published 130 research articles in journals and conferences. He is co-editor of a book Multimedia over Cognitive Radio Networks: Algorithms, Protocols, and Experiments published by the CRC Press. His research has been funded by the U.S. NSF, DOD, DOE, and California Energy Commission.

His research has been funded by the U.S. NSF, DOD, DOE, and California Energy Commission.



John D. Matyjas received his Ph.D. in electrical engineering from State University of New York at Buffalo in 2004. Currently, he is serving as the Connectivity & Dissemination Core Technical Competency Lead at the Air Force Research Laboratory (AFRL) in Rome, NY. His research interests include dynamic multiple-access communications and networking, spectrum mutability, statistical signal processing and optimization, and neural networks. He serves on the IEEE Transactions on Wireless Communications Editorial Advisory Board.

Dr. Matyjas is the recipient of the 2012 IEEE R1 Technology Innovation Award, 2012 AFRL Harry Davis Award for "Excellence in Basic Research," and the 2010 IEEE Int'l Communications Conf. Best Paper Award. He is an IEEE Senior Member, chair of the IEEE Mohawk Valley Signal Processing Society, and member of Tau Beta Pi and Eta Kappa Nu.